Kinetics of the $C_2H_5O_2 + NO_x$ Reactions: Temperature Dependence of the Overall Rate Constant and the $C_2H_5ONO_2$ Branching Channel of $C_2H_5O_2 + NO$

Dana L. Ranschaert, Nicholas J. Schneider, and Matthew J. Elrod*

Department of Chemistry, Hope College, Holland, Michigan 49423

Received: January 28, 2000; In Final Form: April 12, 2000

The temperature dependence of the overall rate constant for the $C_2H_5O_2 + NO$ reaction and the rate constant for the minor branching channel resulting in the production of $C_2H_5ONO_2$ have been measured using the turbulent flow technique with high-pressure chemical ionization mass spectrometry for the detection of reactants and products. The temperature dependence of the overall rate constant for the $C_2H_5O_2 + NO$ reaction was investigated between 299 and 213 K at 100 Torr pressure, and the data was fit to the following Arrhenius expression (with 2 standard deviation error limits indicated): $3.8^{+2.1}_{-1.3} \times 10^{-12}\exp[(290 \pm 110)/T]$ cm^3 molecule^{-1} s^{-1}. The temperature dependence of the overall rate constant agrees well with the current recommendation for atmospheric modeling. The minor reaction channel $C_2H_5O_2 + NO \rightarrow C_2H_5ONO_2$ was directly observed for the first time, and the temperature dependence of the rate constant for this channel was investigated between 298 and 213 K at 100 Torr pressure. The following Arrhenius expression was determined for the minor channel: $1.6^{+4.0}_{-1.2} \times 10^{-15}\exp[(1160 \pm 310)/T]$ cm^3 molecule^{-1} s^{-1}. The Arrhenius expressions for the overall rate and the $C_2H_5ONO_2$ producing channel indicate a branching ratio of about 0.006 at 298 K and 0.02 at 213 K at 100 Torr pressure. The temperature dependence of the overall rate constant for the $C_2H_5O_2 + NO_2$ reaction was also investigated between 299 and 213 K at 100 Torr pressure, and the data was fit to the following Arrhenius expression: $4.7^{+2.0}_{-1.4} \times 10^{-13}\exp[(620 \pm 89)/T]$ cm^3 molecule^{-1} s^{-1}.

Introduction

Alkyl peroxy radicals (RO_2) are important intermediate species formed in the oxidation of alkanes in the atmosphere.[1]

$$RH + OH \rightarrow R + H_2O \quad (1)$$

$$R + O_2 + M \rightarrow RO_2 + M \quad (2)$$

Ozone levels in the atmosphere are directly affected by RO_2 reactions, which themselves are dependent on the levels of the nitrogen oxides (NO_x). Under high NO_x conditions (generally, lower tropospheric urban conditions), RO_2 reactions lead to the production of ozone, the most deleterious constituent of photochemical smog.

$$RO_2 + NO \rightarrow RO + NO_2 \quad (3a)$$

$$NO_2 + h\nu\ (\lambda < 380\ \text{nm}) \rightarrow NO + O \quad (4)$$

$$O + O_2 + M \rightarrow O_3 + M \quad (5)$$

RO_2 can also be temporarily removed from the ozone production cycles by the formation of reservoir species

$$RO_2 + NO + M \rightarrow RONO_2 + M \quad (3b)$$

$$RO_2 + NO_2 + M \leftrightarrow RO_2NO_2 + M \quad (6)$$

Because reaction 3b and the forward reaction 6 remove the radical chain carrier RO_2 from the ozone production cycle, they have a direct effect on the ozone-producing efficiency of the relevant RH/NO_x system. Atkinson and co-workers have developed an empirical relationship for the yield of organic nitrates from reaction 3b from the results of environmental chamber photolysis studies of C_3-C_8 *n*-alkanes.[2] The branching ratio $[k_{3b}/(k_{3a} + k_{3b})]$ is predicted to rise from 0.008 for the methyl case to 0.32 for the *n*-octyl case at 298 K and 760 Torr, thus indicating the importance of the association channel 3b for the larger alkyl peroxy radicals.

Bertman et al. have proposed that the alkyl nitrate branching ratios can be used in regional atmospheric models that determine the air mass age from observations of the relative concentration of alkyl nitrate to the parent alkane. This measurement can serve as a "photochemical clock" since the ratio of alkyl nitrate to the parent alkane increases with air mass age. Using this air mass age, in addition to meteorological back trajectories, can help to identify specific regional ozone production events.[3] Although their method was found to be self-consistent for the secondary C_4 and C_5 nitrates, Bertman et al. found that their model systematically underpredicted measured ethyl nitrate levels by a substantial amount. They speculated that either the branching ratio they had used for ethyl nitrate (0.014, an upper limit estimated earlier for 760 Torr and 298 K by Atkinson et al.[4]) in their model was too low or that there was an ethyl nitrate source other than reaction 3b in the photochemical system. Therefore, it is of interest to directly measure the ethyl nitrate branching ratio under atmospheric conditions.

There have been several previous kinetics investigations of the rate of reaction of $C_2H_5O_2 + NO$.[5−9] It has been well established that reaction 7a

$$C_2H_5O_2 + NO \rightarrow C_2H_5O + NO_2 \quad (7a)$$

is the predominant channel. Because $C_2H_5ONO_2$ has been

* To whom correspondence should be addressed. E-mail: elrod@hope.edu. Telephone: (616) 395-7629. FAX: (616) 395-7118.

10.1021/jp000353k CCC: $19.00
Published on Web 05/23/2000

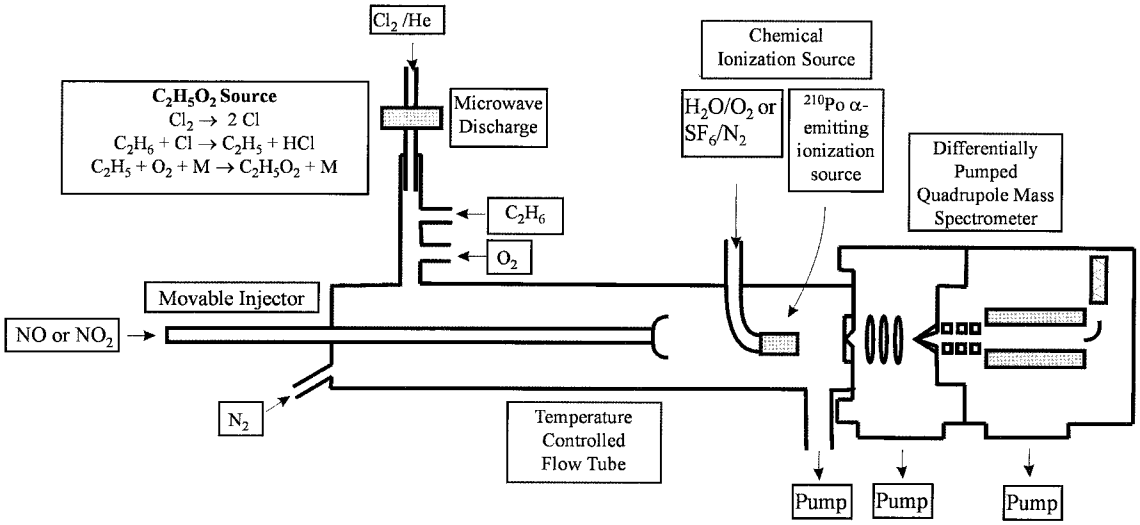

Figure 1. Experimental apparatus.

detected in the atmosphere,[3] it is assumed that reaction 7b

$$C_2H_5O_2 + NO + M \rightarrow C_2H_5ONO_2 + M \qquad (7b)$$

is also kinetically accessible, although no direct laboratory detection of reaction 7b has been previously reported.

In this article we describe our investigation of the kinetics of the $C_2H_5O_2 + NO$ conducted at pressures near 100 Torr and at a range of temperatures extending to those found in the lower stratosphere using a turbulent flow (TF) tube coupled to a high pressure chemical ionization mass spectrometer (CIMS). It has been previously shown that the TF technique can be used to accurately determine the rate constants of reactions at pressures ranging from 50 to 760 Torr and at temperatures as low as 180 K.[10] As in previous kinetics studies of $HO_2 + NO$,[11] $HO_2 + BrO$,[12] $ClO + NO_2$[13] $OH + ClO$,[14,15] and $CH_3O_2 + NO$[16] using the coupled TF−CIMS approach, we are able to directly access atmospheric pressure and temperature conditions and sensitively monitor many of the relevant reactants and products for the $C_2H_5O_2 + NO$ reaction. In the $CH_3O_2 + NO$ work, TF−CIMS kinetics technique was used in the determination of the temperature-dependent overall rate constant and an upper limit for the CH_3ONO_2 producing channel of the $CH_3O_2 + NO$ reaction for pressures and temperatures representative of the upper troposphere.[16] In this article we describe a similar temperature-dependent kinetics investigation of the overall rate (k_7) and the first measurement of the $C_2H_5ONO_2$ producing channel rate (k_{7b}) of the $C_2H_5O_2 + NO$ reaction, as well as the first measurement of the temperature dependence of the rate constant for the reaction of $C_2H_5O_2$ with NO_2

$$C_2H_5O_2 + NO_2 + M \rightarrow C_2H_5O_2NO_2 + M \qquad (8)$$

Experimental Section

Turbulent Fast Flow Kinetics. A schematic of the experimental apparatus is presented in Figure 1 and is similar to that used in our previous study of $CH_3O_2 + NO$ (ref 16). The flow tube was constructed with 2.2 cm i.d. Pyrex tubing and was 100 cm in total length. A large flow of nitrogen carrier gas (approximately 30 STP L min^{-1}) was injected at the rear of the flow tube. The gases necessary to generate $C_2H_5O_2$ were introduced through a 10 cm long 12.5 mm diameter sidearm located at the rear of the flow tube. NO was added via an encased movable injector. The encasement (made from corrugated Teflon tubing) was used so that the injector could be moved to various injector positions without breaking any vacuum seals, as well as to prevent ambient gases from condensing on cold portions of the injector. A fan-shaped Teflon device was placed at the end of the injector in order to enhance turbulent mixing. The polonium-210 alpha-emitting ionization source was placed between the temperature regulated flow tube and the inlet to the CIMS. Most of the flow tube gases were removed at the CIMS inlet by a 31 L s^{-1} roughing pump. All gas flows were monitored with calibrated mass flow meters. The flow tube pressure was measured upstream of the ionization source using a 0−1000 Torr capacitance manometer. The temperature was determined at both the entrance and exit points of the temperature regulated region of the flow tube using Cu−constantan thermocouples.

Reactant Preparation. $C_2H_5O_2$ was generated using the following reactions:

$$C_2H_6 + Cl \rightarrow C_2H_5 + HCl \qquad (9)$$

$$C_2H_5 + O_2 + M \rightarrow C_2H_5O_2 + M \qquad (10)$$

($k_9 = 5.7 \times 10^{-11}$ cm^3 $molecule^{-1}$ s^{-1} and $k_{10} = 7.0 \times 10^{-12}$ cm^3 $molecule^{-1}$ s^{-1} at 100 Torr; all rate constant values quoted are for 298 K values unless otherwise indicated).[17] Chlorine atoms were produced by passing a dilute Cl_2/He mixture through a microwave discharge produced by a Beenakker cavity operating at 50 W. The dilute Cl_2/He mixture was obtained by combining a 2.0 STP L min^{-1} flow of helium (99.999%), which had passed through a silica gel trap immersed in liquid nitrogen, with a 0.5−5.0 STP mL min^{-1} flow of a 1% Cl_2 (99.9%)/He mixture. To generate C_2H_5, the chlorine atoms were then injected into a sidearm and mixed with an excess of C_2H_6 (CP grade, $\sim 10^{13}$ molecules cm^{-3}) in order to ensure that no chlorine atoms were introduced into the main flow. $C_2H_5O_2$ was then produced by the addition of a large excess of O_2 (99.995%; $>1.0 \times 10^{17}$ molecules cm^{-3}) just downstream of the production of C_2H_5. Absolute $C_2H_5O_2$ concentrations (needed to ensure pseudo first-order kinetics conditions and for branching ratio modeling) were determined using two independent methods. The first method involved the measurement of the HCl produced from reaction 9, and the determination of the absolute HCl concentration via calibration of the mass spectrometer signal using a bubbler containing a 20 wt % HCl/H_2O solution kept at 0° C ($p_{HCl} =$ 0.038 Torr).[18] The $C_2H_5O_2$ concentration was then assumed to be the same as the measured HCl concentration. This ap-

proximation is expected to be valid, as the high concentration of O_2 guarantees an extremely fast conversion of C_2H_5 to $C_2H_5O_2$ via reaction 10, and $C_2H_5O_2$ reacts relatively slowly with itself. The second method involved the titration of $C_2H_5O_2$ with NO in the presence of O_2 to produce CH_3CHO:

$$C_2H_5O_2 + NO \rightarrow C_2H_5O + NO_2 \quad (11)$$

$$C_2H_5O + O_2 \rightarrow CH_3CHO + HO_2 \quad (12)$$

($k_{11} = 8.7 \times 10^{-12}$ cm^3 molecule^{-1} s^{-1} and $k_{12} = 1.0 \times 10^{-14}$ cm^3 molecule^{-1} s^{-1})[17] and subsequent calibration of the CH_3CHO mass spectrometer signal. Standard samples were prepared by drawing an appropriate amount of CH_3CHO vapor from a pure liquid sample, followed by mixing with N_2 to make 1% CH_3CHO mixtures appropriate for mass spectrometric calibration. Computer modeling of these titration reactions indicated that not all of the $C_2H_5O_2$ initially present was converted to the stable species, CH_3CHO. This is mainly due to reactions of C_2H_5O with other species in the chemical system (which will be addressed in the discussion section). Therefore, the $C_2H_5O_2$ concentrations were calculated from the CH_3CHO concentrations by explicitly determining the conversion factor (usually ~0.8) from computer modeling using the specific experimental conditions. The NO (CP grade) used in reaction 11 was purified by several freeze/pump/thaw cycles to remove NO_2 impurities. The NO_2/NO ratio of the purified sample was typically less than 1% as determined from CIMS NO_2 detection and calibration methods. For this study, $C_2H_5O_2$ concentrations ranged from 0.5 to 30.0 $\times$ 10^{11} molecules cm^{-3}.

For the overall rate determination for the $C_2H_5O_2$ + NO reaction, NO was purified before use as described above and was added to the flow reactor as a 10% mixture in N_2 through the movable injector. For the overall rate determination for the $C_2H_5O_2$ + NO_2 reaction, the NO_2 was used without further purification and added as a 10% mixture in N_2. NO and NO_2 concentrations used in this study ranged from 0.5 to 60.0 $\times$ 10^{12} molecules cm^{-3}. To ensure pseudo first-order kinetics conditions, NO and NO_2 were kept at levels at least 10 times larger than the $C_2H_5O_2$ levels.

For the low-temperature studies, liquid nitrogen cooled silicone oil was used as the coolant for the jacketed flow tube. Nitrogen carrier gas was precooled by passing it through a copper coil immersed in a liquid N_2 reservoir followed by resistive heating. The temperature was controlled in the reaction region to within 1 K. The pressure was maintained at approximately 100 Torr in order to achieve optimum instrument performance. Pressures below 100 Torr were found to lower the ionization efficiency and pressures above 100 Torr were found to lower the radical production efficiency.

$C_2H_5ONO_2$ Branching Channel Measurements. In these studies, the production of $C_2H_5ONO_2$ from reaction 7b was monitored directly over a reaction time of ~25 ms. Computer modeling was used to extract the rate constant k_{7b} from the observed production of $C_2H_5ONO_2$ and the initial concentrations of all relevant chemical species. As will be discussed in the Results and Discussion section, both the time profile of the $C_2H_5ONO_2$ production and the absolute amount of $C_2H_5ONO_2$ produced over the longest reaction time were used as constraints on the determination of k_{7b}, therefore it was critical that the absolute $C_2H_5ONO_2$ concentrations were determined accurately. Standard samples of $C_2H_5ONO_2$ for mass spectrometric calibration were prepared as follows. $C_2H_5ONO_2$ was prepared by dropwise addition of a solution of 2 mL of 95% H_2SO_4 and 6 mL of 100% C_2H_5OH to an ice-bath cooled solution containing 15 mL of 95% H_2SO_4, 15 mL of 70% HNO_3, and 0.5 g of urea. The solution was stirred for 5 min. The upper organic layer (containing $C_2H_5ONO_2$) was pipetted off and washed with 20 mL of ice-cold distilled water. A separatory funnel was used to drain the lower aqueous layer, and the washing process was repeated several times. The organic layer was then washed with 80 mL of ice-cold 22% NaCl solution and was drained and stored in a volumetric flask at −10° C. The high purity of the $C_2H_5ONO_2$ samples was confirmed by ^{1}H NMR spectroscopy ($\delta_{CH_2} = 4.44$ ppm, and $\delta_{CH_3} = 1.30$ ppm) in $CDCl_3$ solvent. The samples did not undergo degradation over the course of several weeks. Standard samples were prepared by drawing an appropriate amount of $C_2H_5ONO_2$ vapor from the liquid sample, followed by mixing with N_2 to make 1% $C_2H_5ONO_2$ mixtures appropriate for mass spectrometric calibration.

To aid in the detection of the $C_2H_5ONO_2$ product, higher $C_2H_5O_2$ levels were used for the branching ratio measurements than in the determination of the bimolecular rate constant (because $C_2H_5O_2$ is the limiting reagent). The major complication in the branching ratio determination is the side reaction resulting from the reaction of the products of the main channel (reaction 7a) of reaction 7

$$C_2H_5O + NO_2 + M \rightarrow C_2H_5ONO_2 + M \quad (13)$$

($k_{13} = 2.6 \times 10^{-11}$ cm^3 molecule^{-1} s^{-1} at 100 Torr).[17] Reaction 13 is therefore a potential source of $C_2H_5ONO_2$, and experimental conditions must be designed to minimize this relatively fast reaction. By keeping O_2 concentrations very high, computer modeling shows that reaction 12 will consume most of the C_2H_5O produced by reaction 7a and minimize production of $C_2H_5ONO_2$ by reaction 13. To drive the production of $C_2H_5ONO_2$ from reaction 13 down to very low levels, O_2 was used as the carrier gas for the branching ratio experiments, so that the oxygen concentration was nearly equal to the total molecular density (for experiments at 100 Torr total pressure, $[O_2] > 3.0 \times 10^{18}$ molecules cm^{-3}).

Chemical Ionization Mass Spectrometric Detection. Positive ion chemical ionization schemes (with H_3O^+ as the reagent ion) were used to detect $C_2H_5O_2$, CH_3CHO, and $C_2H_5ONO_2$, and negative ion chemical ionization schemes (with SF_6^- as the reagent ion) were used to detect HCl and NO_2 with the quadrupole mass spectrometer. H_3O^+ was produced in the ion source by passing a large O_2 flow (10 STP L min^{-1}) through the polonium-210 alpha-emitting ionization source (with H_2O impurities being sufficiently abundant to produce adequate quantities of reagent ions). SF_6^- was produced in the ion source by passing a large N_2 flow (10 STP L min^{-1}) and 0.1 STP mL min^{-1} of SF_6 through the ionization source. The commercial ionization source consisted of a hollow cylindrical (69 by 12.7 mm) aluminum body with 10 mCurie (3.7×10^8 disintegrations s^{-1}) of polonium-210 coated on the interior walls.

Ions were detected with a quadrupole mass spectrometer housed in a two-stage differentially pumped vacuum chamber. Flow tube gases (neutrals and ions) were drawn into the front chamber through a 0.1 mm aperture, which was held at a potential of ±210 V. The ions were focused by three lenses constructed from 3.8 cm i.d., 4.8 cm o.d aluminum gaskets. The front chamber was pumped by a 6 in. 2400 L s^{-1} diffusion pump. The gases entered the rear chamber through a skimmer cone with a 1.0 mm orifice (held at ±130 V) which was placed approximately 5 cm from the front aperture. The rear chamber was pumped by a 250 L s^{-1} turbomolecular pump. Once the ions passed through the skimmer cone, they were mass filtered and detected with a quadrupole mass spectrometer.

Chemical Ionization Schemes To perform pseudo-first-order rate kinetics studies of the overall rate of reaction 7, a chemical ionization scheme for $C_2H_5O_2$ is required. In our previous study of the $CH_3O_2 + NO$ reaction,[16] we developed the following chemical ionization detection scheme for CH_3O_2 based on the computational thermochemical prediction[19] that CH_3O_2 has a higher proton affinity than H_2O:

$$CH_3O_2 + H_3O^+ \rightarrow CH_3OOH^+ + H_2O \qquad (14)$$

Because the proton affinity of $C_2H_5O_2$ is expected to be very similar to CH_3O_2, we successfully attempted to detect $C_2H_5O_2$ with the analogous reaction

$$C_2H_5O_2 + H_3O^+ \rightarrow C_2H_5OOH^+ + H_2O \qquad (15)$$

Depending on the amount of the water in the flow system, $C_2H_5O_2$ was detected as $C_2H_5OOH^+(H_2O)_n$, where n was typically 2 or 3.

To perform branching ratio measurements for reaction 7b, chemical ionization schemes are needed for CH_3CHO, HCl (for the two $C_2H_5O_2$ absolute concentration determination methods described above), NO_2 (to assess the purity of the NO used and any potential interference from side reaction 13), and for the product $C_2H_5ONO_2$. In a previous study, acetaldehyde was found to react quickly with H_3O^+

$$CH_3CHO + H_3O^+ \rightarrow CH_3CHOH^+ + H_2O \qquad (16)$$

($k_{16} = 3.6 \times 10^{-9}$ cm^3 molecule^{-1} s^{-1}).[20] Again, depending on the amount of the water in the flow system, CH_3CHO was detected as $CH_3CHOH^+(H_2O)_n$, where n was typically 2 or 3. HCl and NO_2 were detected using previously reported SF_6^- chemical ionization schemes

$$HCl + SF_6^- \rightarrow F^-HCl + SF_5 \qquad (17)$$

$$NO_2 + SF_6^- \rightarrow NO_2^- + SF_6 \qquad (18)$$

($k_{17} = 4.2 \times 10^{-10}$ cm^3 molecule^{-1} s^{-1} and $k_{18} = 1.4 \times 10^{-10}$ cm^3 molecule^{-1} s^{-1}).[21] Previously, we found that CH_3ONO_2 reacted with H_3O^+, but at a rate that was too slow for sensitive mass spectrometric detection.[16] In this study, it was determined that $C_2H_5ONO_2$ reacts very quickly with H_3O^+

$$C_2H_5ONO_2 + H_3O^+ \rightarrow C_2H_5ONO_2{\bullet}H^+ + H_2O \qquad (19)$$

such that very high sensitivity could be achieved for the detection of this important product. Again, depending on the amount of the water in the flow system, $C_2H_5ONO_2$ was detected as $C_2H_5ONO_2{\bullet}^+(H_2O)_n$, where n was typically 2 or 3. The detection sensitivity for $C_2H_5ONO_2$ was estimated to be about 100 ppt at 100 Torr.

Results and Discussion

Overall Rate Constant Determination. Bimolecular rate constants were obtained via the usual pseudo first-order approximation method, using NO or NO_2 as the excess reagent. Typical $C_2H_5O_2$ decay curves as a function of injector distance are shown in Figure 2 for the NO kinetics measurements. The first-order rate constants obtained from fitting the $C_2H_5O_2$ decay curves were plotted against [NO] in order to determine the bimolecular rate constant, as shown in Figure 3. This approach for determining bimolecular rate constants assumes that deviations from the plug flow approximation (molecular velocities are equal to the bulk flow velocity) are negligible. Under the conditions present in our turbulent flow tube (Reynolds no. > 2000), Seeley et al. estimated that these deviations result in apparent rate constants which are at most 8% below the actual values.[22] Hence, the flow corrections were neglected as they are smaller than the sum of the other likely systematic errors in the measurements of gas flows, temperature, detector signal, and pressure. Considering such sources of error, we estimate that rate constants can be determined with an accuracy of ±30% (2σ).

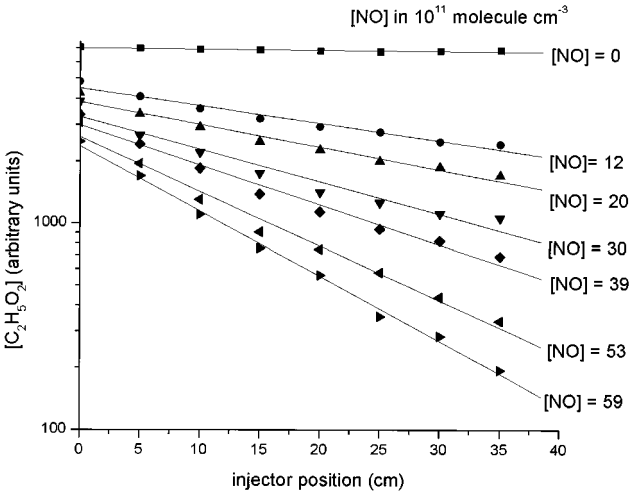

Figure 2. Pseudo first-order $C_2H_5O_2$ decay curves for the $C_2H_5O_2 + NO$ reaction at 100 Torr, 253 K, and 1070 cm s^{-1} velocity.

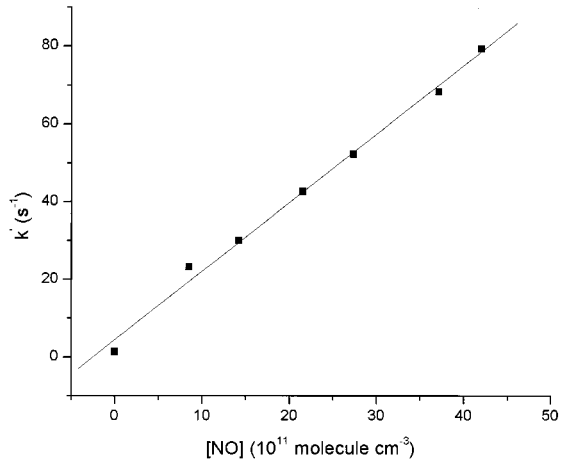

Figure 3. Determination of the overall bimolecular rate constant for the $C_2H_5O_2 + NO$ reaction from data in Figure 2.

We performed several determinations of the rate constant at 100 Torr and 299 K for the $C_2H_5O_2 + NO$ reaction (see Table 1 for a complete list of experimental conditions and measured rate constants) and arrived at the mean value of $k = (10.1 \pm 0.9) \times 10^{-12}$ cm^3 molecule^{-1} s^{-1}; the uncertainty represents the two standard deviation statistical error in the data and is not an estimate of systematic errors. Our room-temperature rate constant is in excellent agreement with previous studies[5-9] and thus with the JPL recommended value for atmospheric modeling.[17]

Temperature Dependence of the Overall Rate Constant (k_7) for $C_2H_5O_2 + NO$. We performed several measurements at 100 Torr pressure and at temperatures between 299 and 213 K in order to establish the temperature dependence of the rate constant for conditions relevant to the upper troposphere (and lower stratosphere). The rate constant increased by approxi-

TABLE 1: Overall Rate Constant Data for the $C_2H_5O_2$ + NO Reaction at 100 Torr Pressure

temperature (K)	velocity (cm s^{-1})	Reynolds no.	k_7[a] (10^{-12} cm^3 $molecule^{-1}$ s^{-1})
299	1210	2110	9.6 ± 1.1
299	1190	2230	11.1 ± 0.7
299	1150	2210	9.6 ± 1.5
273	1150	2540	10.2 ± 1.0
263	1150	2510	13.8 ± 4.2
263	1075	2490	11.8 ± 1.6
258	1075	2630	11.0 ± 0.7
253	1070	2680	12.4 ± 0.7
248	1060	2660	13.1 ± 4.0
248	970	2560	12.1 ± 2.2
243	930	2630	12.2 ± 2.7
238	970	2630	14.6 ± 3.1
238	1050	2710	13.3 ± 6.2
233	980	2830	12.2 ± 1.7
233	980	2910	15.4 ± 1.3
228	1075	3230	13.9 ± 1.3
223	1130	3540	15.0 ± 3.5
213	1200	3740	13.4 ± 1.2

[a] Stated error is 2σ.

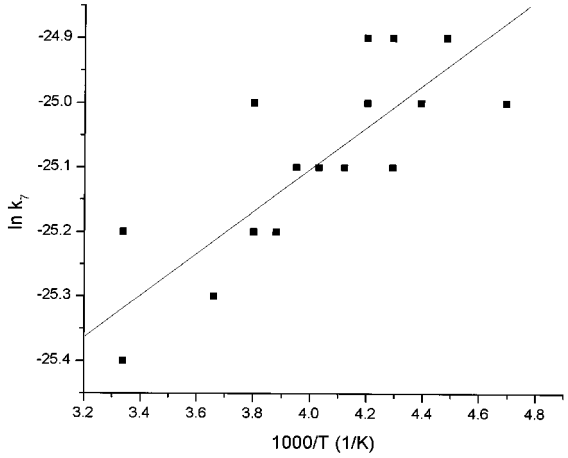

Figure 4. Arrhenius plot of the temperature dependence of the overall rate constant for the $C_2H_5O_2$ + NO reaction.

TABLE 2: Overall Rate Constant Data for the $C_2H_5O_2$ + NO_2 Reaction at 100 Torr Pressure

temperature (K)	velocity (cm s^{-1})	Reynolds no.	k_8[a] (10^{-12} cm^3 $molecule^{-1}$ s^{-1})
299	1140	2070	2.77 ± 0.28
297	1090	2080	3.38 ± 0.20
283	1080	2190	4.10 ± 0.39
283	1070	2190	4.01 ± 0.63
273	1020	2210	4.89 ± 0.57
273	1000	2180	4.76 ± 0.54
263	969	2250	5.06 ± 2.10
263	962	2240	4.42 ± 0.56
253	1010	2540	4.43 ± 0.88
253	989	2500	5.64 ± 0.46
243	946	2430	6.49 ± 1.23
243	943	2450	6.33 ± 1.97
233	961	2670	6.31 ± 1.48
233	953	2760	7.00 ± 0.54
228	1040	3090	7.07 ± 0.52
223	1060	3390	6.61 ± 0.83
223	969	3000	7.89 ± 0.52
213	1030	3420	7.95 ± 0.33
213	1080	3580	8.48 ± 0.79

[a] Stated error is 2σ.

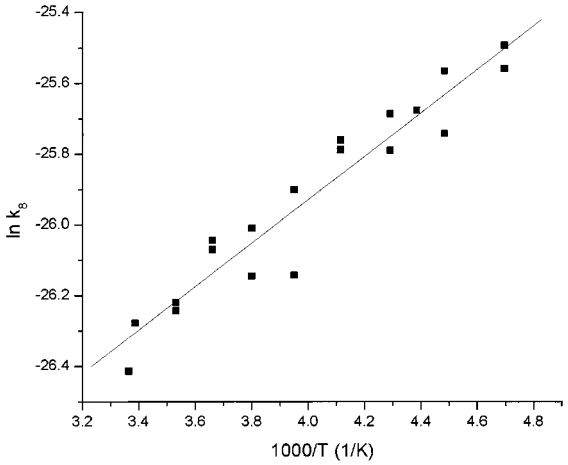

Figure 5. Arrhenius plot of the temperature dependence of the overall rate constant for the $C_2H_5O_2$ + NO_2 reaction.

mately 50% as the temperature was lowered over this range. From the data listed in Table 1 and plotted in Figure 4, we obtained the Arrhenius expression $k(T) = 3.8^{+2.1}_{-1.3} \times 10^{-12}$-exp[(290 ± 110)/$T$] cm^3 $molecule^{-1}$ s^{-1}. Our results are in good agreement with the two previous temperature dependence studies[5,6] and the JPL recommended value for atmosphere modeling.[17]

Temperature Dependence of the Overall Rate Constant (k_8) for $C_2H_5O_2$ + NO_2. In a manner similar to our measurement for the $C_2H_5O_2$ + NO reaction, we performed several measurements at 100 Torr pressure and at temperatures between 299 and 213 K in order to detail the temperature dependence of the overall rate constant for $C_2H_5O_2$ + NO_2. The rate constant increased approximately 3-fold as the temperature was lowered over this range. From the data listed in Table 2 and plotted in Figure 5, we obtain the Arrhenius expression $k(T) = 4.7^{+2.0}_{-1.4} \times 10^{-13}$exp[(620 ± 89)/$T$] cm^3 $molecule^{-1}$ s^{-1}. To our knowledge, there has been only one previous estimate of the pressure dependence of this rate constant and no temperature dependence study for this reaction. Elfers et al.[23] measured the rate of the $C_2H_5O_2$ + NO_2 reaction relative to the $C_2H_5O_2$ + NO reaction at 254 K and found that the reaction rate increased from $0.21 \times k_7$ at 7.5 Torr, to $0.50k_7$ at 75 Torr to $0.81k_7$ at 746 Torr. Using our value for k_7 at 254 K as calculated from the Arrhenius expression, the relative rate constants of Elfers et al. can be converted to the following absolute rate constants: k_8 (7.5 Torr) = 2.5×10^{-12} cm^3 $molecule^{-1}$ s^{-1}, k_8 (75 Torr) = 6.0×10^{-12} cm^3 $molecule^{-1}$ s^{-1}, and k_8 (750 Torr) = 9.6×10^{-12} cm^3 $molecule^{-1}$ s^{-1}. Our value for k_8 at 100 Torr and 254 K (as calculated from Arrhenius expression above) is 5.4×10^{-12} cm^3 $molecule^{-1}$ s^{-1}, which is reasonable agreement with the measurement of Elfers et al. at 75 Torr. We attempted to detect the $C_2H_5O_2NO_2$ product from reaction 8 using the $H^+(H_2O)_n$ chemical ionization proton transfer reaction successfully used for $C_2H_5O_2$, CH_3CHO and $C_2H_5ONO_2$ detection. However, we did not observe the ion corresponding to the expected proton transfer product. This result most likely indicates that $C_2H_5O_2$-NO_2 has a lower proton affinity than water, rather than indicating that $C_2H_5O_2NO_2$ is not a product of reaction 8.

$C_2H_5ONO_2$ Branching Ratio Determination. We were able to observe the production of very small concentrations of C_2H_5-ONO_2 ($\sim 3.0 \times 10^9$ molecules cm^{-3}) over the reaction time ($\sim$25 ms), which we have positively identified as coming from reaction 7b. In Figure 6, the $C_2H_5ONO_2$ rise (squares) has been overlaid on the background signal (circles) to demonstrate that the $C_2H_5ONO_2$ rise is significantly larger than the $\pm 2\sigma$ level of the background signal. Under the optimal experimental

TABLE 3: Kinetics Parameters for Branching Ratio Determination

reaction[a]	A ($cm^3\ s^{-1}$ molecule^{-1})	E_a/R (K)	k_o^{300} ($cm^6\ s^{-1}$ molecule^{-2})	m	k_∞^{300} ($cm^3\ s^{-1}$ molecule^{-1})	n
$C_2H_5O_2 + NO \rightarrow$ products (this work)	3.8×10^{-12}	−290				
$2\ C_2H_5O_2 \rightarrow$ products	6.8×10^{-14}	0				
$C_2H_5O_2 + NO_2 \rightarrow C_2H_5O_2NO_2$(IUPAC)			4.0×10^{-28}	6.2	8.8×10^{-12}	0
$C_2H_5O_2 + HO_2 \rightarrow CH_3CHO + H_2O + O_2$(IUPAC)	3.8×10^{-13}	−900				
$C_2H_5 + O_2 \rightarrow C_2H_5O_2$			1.5×10^{-28}	3	8.0×10^{-12}	0
$C_2H_5O + O_2 \rightarrow CH_3CHO + HO_2$(IUPAC)	6.3×10^{-14}	550				
$C_2H_5O + NO \rightarrow C_2H_5ONO$			2.8×10^{-27}	4	5.0×10^{-11}	1
$C_2H_5O + NO_2 \rightarrow C_2H_5ONO_2$			2.0×10^{-27}	4	2.8×10^{-11}	1
$HO_2 + NO \rightarrow OH + NO_2$	3.5×10^{-12}	−250				
$HO_2 + OH \rightarrow H_2O + O_2$	4.8×10^{-11}	−250				
$OH + OH \rightarrow H_2O_2$			6.2×10^{-31}	1	2.6×10^{-11}	0
$OH + NO \rightarrow HONO$			7.0×10^{-31}	2.6	3.6×10^{-11}	0.1
$OH + NO_2 \rightarrow HNO_3$			2.5×10^{-30}	4.4	1.6×10^{-11}	1.7
$OH + CH_3CHO \rightarrow CH_3CO + H_2O$	5.6×10^{-12}	−270				
$OH + C_2H_6 \rightarrow C_2H_5 + H_2O$	8.7×10^{-12}	1070				

[a] All data from the JPL compilation (DeMore, W.B.; Sander, S. P.; Howard, C. J; Ravishankara, A. R.; Golden, D. M.; Kolb, C. E.; Hampson, R. F; Kurylo, M. J.; Molina, M. J. *Chemical Kinetics and Photochemical Data for Use in Stratospheric Modeling*; JPL Publication 97-4; Jet Propulsion Laboratory: Pasadena, CA, 1997), unless specifically indicated as from the IUPAC compilation (Atkinson, R.; Baulch, D. L.; Cox, R. A.; Hampson, R. F.; Kerr, J. A.; Rossi, M. J.; Troe, J. *Summary of Evaluated Kinetic Data for Atmospheric Chemistry*; IUPAC Subcommittee on Gas Kinetic Data Evaluation for Atmospheric Chemistry: Cambridge, UK, 1999 (http://www.iupac-kinetic.ch.cam.ac.uk). Pressure-independent rate constants calculated from $k(T) = Ae^{-E_a/RT}$. Pressure-dependent rate constants calculated from $k([M],T) = ((k_o(T)[M])/(1 + k_o(T)[M]/k_\infty(T)))0.6^{(1+(\log_{10}((k_o(T)[M])/(k_\infty(T))))^2)^{-1}}$ where $k_o(T) = k_o^{300}(T/300)^{-n}$ and $k_\infty(T) = k_\infty^{300}(T/300)^{-m}$.

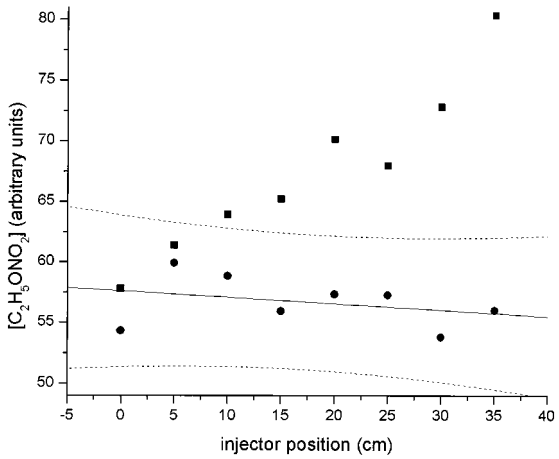

Figure 6. Observed production of $C_2H_5ONO_2$ from reaction 7b (squares) Above the $C_2H_5ONO_2$ Background level (circles) as a function of injector distance. A least-squares fit to the background level was performed, and the dotted lines represent the 2σ level. This data set was obtained under the following conditions: $P = 100$ Torr, $T = 223$ K, velocity = 925 cm s^{-1}, Reynolds no. = 2820, $[C_2H_5O_2]_0 = 1.8 \times 10^{12}$ molecules cm^{-3}, $[NO]_0 = 3.3 \times 10^{12}$ molecules cm^{-3}.

conditions ($[C_2H_5O_2] \sim 2.0 \times 10^{12}$ molecules cm^{-3}, $[NO] \sim 1.0 \times 10^{13}$ molecules cm^{-3}, and $[O_2] \sim 3.0 \times 10^{18}$ molecules cm^{-3}) kinetics modeling shows that side reactions can produce concentrations of $C_2H_5ONO_2$ that are on the order of the detection level of the instrument ($\sim 5.0 \times 10^8$ molecules cm^{-3}) and are significantly less than the actual $C_2H_5ONO_2$ observed. Table 3 contains a list of the reactions used in the modeling. An inspection of Table 3 indicates that only one side reaction directly produces $C_2H_5ONO_2$:

$$C_2H_5O + NO_2 + M \rightarrow C_2H_5ONO_2 + M \qquad (13)$$

However, this reaction is significant in that the reactants are the products of dominant reaction channel for $C_2H_5O_2 + NO$. As mentioned in the Experimental Section, oxygen was used as the carrier gas in the branching ratio experiments in order to achieve very high O_2 concentrations. The high O_2 concentrations favor the following reaction

$$C_2H_5O + O_2 \rightarrow CH_3CHO + HO_2 \qquad (12)$$

which effectively scavenges C_2H_5O from the system. Although the HO_2 product formed from this reaction could conceivably lead to the reforming of $C_2H_5O_2$ (and thus C_2H_5O) in the system via the following reactions

$$HO_2 + NO \rightarrow OH + NO_2 \qquad (20)$$

$$OH + C_2H_6 \rightarrow C_2H_5 + H_2O \qquad (21)$$

$$C_2H_5 + O_2 + M \rightarrow C_2H_5O_2 + M \qquad (10)$$

($k_{20} = 8.1 \times 10^{-12}$ cm^3 molecule^{-1} s^{-1} and $k_{21} = 7.0 \times 10^{-12}$ cm^3 molecule^{-1} s^{-1} at 100 Torr), computer modeling shows that the OH product from reaction 20 primarily reacts with NO and NO_2 (rather than C_2H_6), to form HONO and HNO_3, respectively, which are relatively unreactive under the flow tube conditions.

Computer modeling was used to extract a rate constant for reaction 7b by fitting the observed $C_2H_5ONO_2$ production. The actual time profile of the $C_2H_5ONO_2$ production, as well as the total production of $C_2H_5ONO_2$ over the total reaction time were used as constraints in the fitting process. The latter constraint is useful in that the competing side reaction 13 approaches completion faster than the desired reaction 7b, such that the proportion of $C_2H_5ONO_2$ that has been produced by reaction 7b increases as longer reaction times are achieved. The model input included the concentrations of $C_2H_5O_2$, NO, and all precursors. Table 4 contains a list of the initial conditions and calculated rate constants (k_{7b}) for the branching ratio experiments. Figure 7 demonstrates the sensitivity of the fitted k_{7b} value to the actual kinetics data collected. The fitted k_{7b} value is subject to error arising from experimental uncertainties, as well as uncertainties in the rate constants used in the modeling process. As stated earlier, we believe that the relevant experimental uncertainty for a rate constant determination with this apparatus is on the order of 30%, although the uncertainty may be somewhat higher due to the fact that the branching ratio

TABLE 4: Branching Ratio Data for the $C_2H_5O_2$ + NO Reaction at 100 Torr Pressure

T (K)	$[C_2H_5O_2]_0$ (10^{11} molecule cm^{-3})	$[NO]_0$ (10^{11} molecule cm^{-3})	k_{7b} (10^{-14} cm^3 molecule^{-1} s^{-1})	branching ratio $k_{7b}/(k_{7a}+k_{7b})$
298	23	110	6.6	0.0065
298	23	120	5.6	0.0055
298	23	130	5.6	0.0055
273	23	82	12	0.0109
263	14	75	14	0.0122
263	14	62	16	0.0139
253	14	63	22	0.0183
253	14	60	25	0.0208
243	20	86	20	0.0159
243	17	93	23	0.0182
233	19	34	26	0.0196
223	18	44	20	0.0143
223	18	33	20	0.0143
223	18	45	28	0.0200
213	19	28	32	0.0215

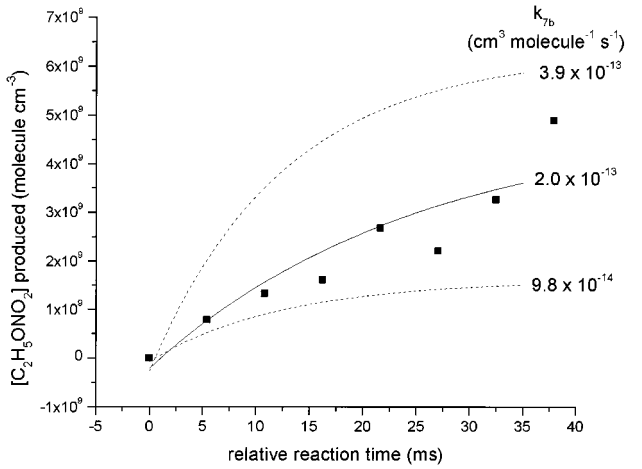

Figure 7. Sensitivity of fitted value of k_{7b} to branching ratio data (given in Figure 6).

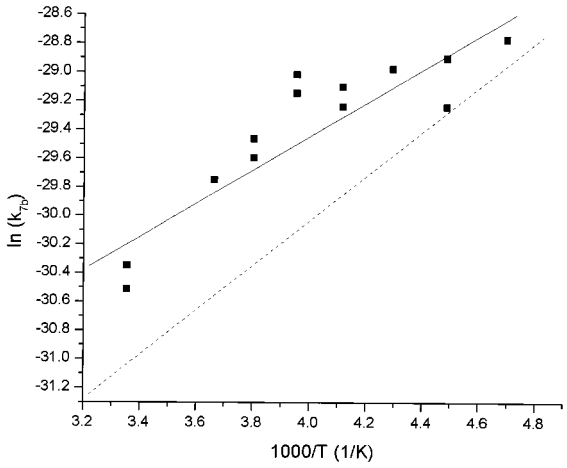

Figure 8. Arrhenius plot of the temperature dependence of the rate constant of the $C_2H_5ONO_2$ branching channel (squares and solid line) and prediction from Atkinson model[2] (dashed line) at 100 Torr pressure.

measurements are being made very close to the detection level of the instrument. In addition, the branching ratio method requires the added step of titration and calibration experiments needed to determine $[C_2H_5O_2]_0$. The uncertainty in the rate constant for reaction 13 is expected to play the largest role in the propagation of rate constant uncertainties through our fitting process. According to the JPL database,[17] the uncertainty in k_{13} is only 15% (because we are operating at the high-pressure limit for this reaction). Propagating this value through our model indicates that this uncertainty has a minor effect (less than 10%) on our fitted value for k_{7b}. Therefore, we estimate the total error to be approximately 50% for the branching ratio measurements.

We performed several measurements of the branching ratio for $C_2H_5O_2$ + NO at temperatures between 213 and 298 K in order to establish the temperature dependence of the rate constant k_{7b} for conditions relevant to the upper troposphere. From the data listed in Table 4 and plotted in Figure 8, we obtained the Arrhenius expression $k_{7b}(T) = 1.6^{+4.0}_{-1.2} \times 10^{-15}$-exp[$(1160 \pm 310)/T$] cm^3 molecule^{-1} s^{-1}. Again, the uncertainty represents the two standard deviation statistical error in the data and is not an estimate of systematic errors (which are discussed above). The branching ratios $[k_{7b}/(k_{7a} + k_{7b})]$ reported in Table 4 were calculated using the measured Arrhenius expression for the overall rate constant k_7 ($k_{7a} + k_{7b}$). The branching ratios range from about 0.006 at 298 K to 0.02 at 213 K, indicating the increased importance of the $C_2H_5ONO_2$-producing channel at lower temperatures. Because the $C_2H_5ONO_2$-producing channel is almost certainly pressure-dependent, it would be of interest to attempt to establish the pressure dependence of the rate constant. However, because the measurements made at 100 Torr were barely within the detection limit of the instrument, it was not surprising that we were unable to obtain sufficient sensitivity to pursue experiments at pressures other than 100 Torr.

There have been no previous measurements of the rate constant for reaction 7b. However, all but one of the rate constant determinations previously reported in the literature were obtained by following the production of NO_2 (refs 6, 8, and 9) or C_2H_5O (ref 7) and thus were measurements of k_{7a}, rather than the overall rate constant k_7. The fact that these measurements of k_{7a} are in good agreement with the only previous measurement of k_7 (ref 5) and the present result for k_7 indicates that the value k_{7b} must be quite small, which is consistent with the present results. The model of Atkinson and co-workers,[2] which is based on measured C_3-C_8 alkyl nitrate branching ratios, can be used to predict a value for k_{7b}. The results from this model are plotted with the experimental results in Figure 8. Although the temperature dependence for k_{7b} is well predicted by the model, the absolute experimental rate constants are consistently higher than the model predictions.

As discussed in the Introduction, the ethyl nitrate-based air mass age model of Bertman et al.[3] used a value for k_{7b} derived from the Atkinson work.[4] Therefore, our finding that k_{7b} is somewhat larger than predicted from the Atkinson model could potentially provide an explanation for the Bertman et al. result that their air mass age model systematically underpredicted $C_2H_5ONO_2$ levels in the atmosphere. However, if one assumes

that reaction 7b is the only source of $C_2H_5ONO_2$ in the atmosphere, measured $[C_2H_5ONO_2]/[C_2H_6]$ ratios can be used (via the Bertman et al. model) to predict the branching ratio ($\beta = k_{7b}/k_7$) for reaction 7b:

$$\beta = \frac{[C_2H_5ONO_2]_{atm}}{[C_2H_6]_{atm}} \times \frac{k_B - k_A}{k_A} \frac{1}{(1 - e^{(k_A - k_B)t})} \quad (22)$$

where k_A is the pseudo first-order rate constant for the rate-limiting $OH + C_2H_6$ step in the mechanism that eventually leads to $C_2H_5ONO_2$ production (2.68×10^{-7} s^{-1}), k_B is the pseudo first-order rate constant for the conversion of $C_2H_5ONO_2$ into other products (1.11×10^{-6} s^{-1}), and t is the air mass age. Using eq 22, a $[C_2H_5ONO_2]/[C_2H_6]$ value of 0.002 and an air mass age of 0.5 days (based on measurements made by Bertman et al. at Kinterbish, Alabama) we calculate an "atmospherically inferred" branching ratio of 0.17. Therefore, although our laboratory findings indicate a higher branching ratio ($\beta = 0.006$ at 100 Torr and 298 K) than indicated by the empirical relationship of Atkinson et al. ($\beta = 0.003$ at 100 Torr and $\beta = 0.014$ at 760 Torr and 298 K), our value is still much lower than the value inferred from atmospheric measurements and the Bertman et al. model ($\beta \sim 0.17$ at ~760 Torr and ~298 K) which assumes $C_2H_5ONO_2$ production from reaction 7b only. This result suggests that ethyl nitrate sources other than reaction 7b are operative in the atmosphere.

Conclusions

The results presented here represent the first measurement of a $C_2H_5ONO_2$ producing channel from the $C_2H_5O_2 + NO$ reaction, as well as measurements of the temperature dependence of the overall rate constant for the reactions of $C_2H_5O_2$ with NO and NO_2. The branching ratio $[k_{7b}/(k_{7a} + k_{7b})]$ at 100 Torr pressure for $C_2H_5ONO_2$ formation was determined to be about 0.006 at 298 K and was found to increase to about 0.02 at 213 K. Although the temperature dependence of the rate constant k_{7b} was fairly accurately predicted by extrapolating from a model based on organic nitrate formation from C_3-C_8 hydrocarbon systems,[2] our absolute rate constants are systematically higher than the model results. Our experimental results should improve the reliability of models[3] that use $C_2H_5ONO_2$ formation as a measure of air mass age in the tracking of ozone-forming pollution sources. Our measurement of the temperature dependence of the overall rate constant for the $C_2H_5O_2 + NO$ reaction was found to be in good agreement with the JPL recommendation.[17] We also performed the first thorough temperature dependence (at 100 Torr pressure) study of the overall rate constant for the $C_2H_5O_2 + NO_2$ reaction, and reasonable agreement was found with an earlier pressure dependence study performed at 254 K.[23] This work should help improve modeling of ozone formation arising from ethane/NO_x chemistry by placing more stringent constraints on the formation of $C_2H_5ONO_2$ and by helping to establish temperature-dependent rate constants for the reactions of $C_2H_5O_2$ with NO and NO_2 for tropospheric pressure and temperature conditions.

Acknowledgment. This research was funded by grants from the Camille and Henry Dreyfus Foundation, American Chemical Society—Petroleum Research Fund, Research Corporation, and the National Science Foundation (Grant ATM-9874752).

References and Notes

(1) Brasseur, G. P.; Orlando, J. J.; Tyndall, G. S. *Atmospheric Chemistry and Global Change*; Oxford University Press: New York, 1999.
(2) Atkinson, R.; Carter, W. P. L.; Winer, A. M. *J. Phys. Chem.* **1983**, *87*, 2012.
(3) Bertman, S. B.; Roberts, J. M.; Parrish, D. D.; Buhr, M. P.; Goldan, P. D.; Kuster, W. C.; Fehsenfeld, F. C.; Montzka, S. A.; Westberg, H. *J. Geophys. Res.* **1995**, *100*, 22805.
(4) Atkinson, R.; Aschmann, S. M.; Carter, W. P. L.; Winer, A. M.; Pitts, J. N. *J. Phys. Chem.* **1982**, *86*, 4563.
(5) Eberhard, J.; Howard, C. J. *Int. J. Chem. Kinet.* **1996**, *28*, 731.
(6) Maricq, M. M.; Szente, J. J. *J. Phys. Chem.* **1996**, *100*, 12374.
(7) Daele, V.; Ray, A.; Vassalli, I.; Poulet, G.; Le Bras, G. *Int. J. Chem. Kinet.* **1995**, *27*, 1121.
(8) Sehested, J.; Nielsen, O. J.; Wallington, T. J. *Chem. Phys. Lett.* **1993**, *213*, 457.
(9) Plumb, I. C.; Ryan, K. R.; Steven, J. R.; Mulcahy, M. F. R. *Int. J. Chem. Kinet.* **1982**, *14*, 183.
(10) Seeley, J. V.; Jayne, J. T.; Molina, M. J. *Int. J. Chem. Kinet.* **1993**, *25*, 571.
(11) Seeley, J. V.; Meads, R. F.; Elrod, M. J.; Molina, M. J. *J. Phys. Chem.* **1996**, *100*, 4026.
(12) Elrod, M. J.; Meads, R. F.; Lipson, J. B.; Seeley, J. V.; Molina, M. J. *J. Phys. Chem.* **1996**, *100*, 5808.
(13) Percival, C. J.; Smith, G. D.; Molina, L. T.; Molina, M. J. *J. Phys. Chem.* **1997**, *101*, 8830.
(14) Lipson, J. B.; Elrod, M. J.; Beiderhase, T.; Molina, L. T.; Molina, M. J. *Faraday Trans.* **1997**, *93*, 2665.
(15) Lipson, J. B.; Beiderhase, T. W.; Molina, L. T.; Molina, M. J.; Olzmann, M. *J. Phys. Chem.* **1999**, *103*, 6540.
(16) Scholtens, K. W.; Messer, B. M.; Cappa, C. D.; Elrod, M. J. *J. Phys. Chem.* **1999**, *103*, 4378.
(17) DeMore, W.B.; Sander, S. P.; Howard, C. J.; Ravishankara, A. R.; Golden, D. M.; Kolb, C. E.; Hampson, R. F.; Kurylo, M. J.; Molina, M. J. *Chemical Kinetics and Photochemical Data for Use in Stratospheric Modeling*; JPL Publication 97-4; Jet Propulsion Laboratory: Pasadena, CA, 1997.
(18) Fritz, J. J.; Fuget, C. R. *Chem. Eng. Data Ser.* **1956**, *1*, 10.
(19) Messer, B. M.; Stielstra, D. E.; Cappa, C. D.; Scholtens, K. W.; Elrod, M. J. *Int. J. Mass Spectrom.* **2000**, *197*, 219.
(20) Adams, N. G.; Smith, D.; Grief, D. *Int. J. Mass Spectrom. Ion Phys.* **1978**, *26*, 405.
(21) Huey, L. G.; Hanson, D. R.; Howard, C. J. *J. Phys. Chem.* **1995**, *99*, 5001.
(22) Seeley, J. V. Experimental Studies of Gas-Phase Radical Reactions Using the Turbulent Flow Tube Technique. Ph.D. Thesis, Massachusetts Institute of Technology, 1994.
(23) Elfers, G.; Zabel, F.; Becker, K. H. *Chem. Phys. Lett.* **1990**, *168*, 14.